Anomalous rainfall and associated atmospheric circulation in the north-east Spanish Mediterranean area and its relationship to sediment fluidization events in a lake

Marianna Soler, Teresa Serra and Jordi Colomer

Group of Environmental Physics, Physics Department, University of Girona, 17071 Girona, Spain

Romualdo Romero

Meteorology Group, Physics Department, University of the Balearic Islands, 07122 Palma de Mallorca, Spain

Corresponding author address:

marianna.soler@udg.es

Group of Environmental Physics, Department of Physics, University of Girona, 17071 Girona, Spain

Acknowledgments

Precipitation data were provided by the ‘Instituto Nacional de Meteorologia’, stations of Jafre, Les Planes d’Hostoles and Castelló d’Empúries. We also would like to thank the people in charge of the meteorological stations of Darnius and Banyoles. The authors are grateful to captain Joan Corominas for the outstanding help and support in the field campaigns in Lake Banyoles. Also to Josep Pasqual (meteorological station of L’Estartit) for providing some of the temperature data in basin B2. The funds for this research were provided by the ‘Ministerio de Ciencia y Tecnología’ (MCYT) projects REN2001-2239/HID and CGL 2004-02027.

Abstract

This study investigates the sediment fluidizations of confined bed-sediments in the last nineteen years (1986-2004) in the basins of Lake Banyoles, located in the north-east of Spain, where water enters mainly through subterranean springs. The sediment fluidization events are studied in basin B2 where fluctuations in the vertical migration of sediment present episodic behavior as a result of episodic rainfall in the area. The initiation of the fluidization events takes place when the monthly rainfall is ~ 2. 7 times greater than the mean monthly rainfall of the rainiest months in the area, especially in spring (April and May), in the months of autumn and in December. Results show that the sediment fluidization in B2 remained in suspension in the 39.9% of the whole historical record. The rainfall, in turn, is associated with six main atmospheric circulation patterns among the 19 fundamental circulations that emerged in an earlier study focused on significant rainfall days in Mediterranean Spain. The 19 circulation types were derived in terms of the geopotential fields at 925 and 500 hPa as provided by the ECMWF gridded data during the period 1984-1993. They comprise a wide variety of flows over the Iberian peninsula, with marked seasonal distributions and a clear distinction between Atlantic and western Mediterranean disturbances. In this study an analogue procedure is used to classify each of the 1970-2002 daily atmospheric states, as represented by the ECMWF reanalysis data, within the 19 circulation types or as insignificant (not rainy) days. The results are then used to construct some statistics aimed at comparing the occurrence of the circulation types during the fluidization periods with their occurrence in the monthly climatology: the Atlantic types AP3, AP4 and AP9, and the Mediterranean types AP8, AP14 and AP19 are identified as the most frequent during the sediment fluidization events and represent 64% of the days with significant rainfall in the months of initiation of the fluidization events. Also, the torrential rainfall episodes within these months are associated to five out of the six

atmospheric patterns (AP3, AP4, AP8, AP14 and AP19) with a 36.1% occurrence of the Mediterranean types associated with disturbances located near or over the southern Iberian Peninsula.

Introduction

Both the spatial and temporal variability of ecological parameters are usually connected to the variability of synoptic atmospheric patterns and certain environmental parameters. In his book, Yarnal (1993) offers multiple examples of synoptic classifications, ranging from subjective manual classifications to outputs from eigenvector-based techniques. Worked examples are used to determine how well these classifications relate to four environmental scenarios in the Pennsylvania area (urban air quality, acid rain, agriculture and fluvial hydrology). Bonell and Summer (1992) establish, using S-mode PCA and CA, the main daily precipitation affinity areas for Wales according to surface wind direction. Regional and North Atlantic atmospheric circulation (represented by the North Atlantic Oscillation) have a remarkable impact on aquatic systems, based on effects on water temperature, ice phenology (Blenckner and Chen 2003, Livingstone 1999, Omstedt and Chen 2001), phytoplankton spring blooms (Blenckner and Chen 2003, Gerten and Adrian 2000, Weyhenmeyer et al 1999), and nitrate, dissolved reactive phosphorous and chlorophyll concentrations (George et al. 2004), although also depending on different thermal lake structures and mixing regimes (Gerten and Adrian 2001).

The Spanish Mediterranean area (Figure 1) possesses a rather complex topography. It is influenced by both Atlantic low pressure systems (notably west and north of the area) and by Mediterranean disturbances (in the eastern part), and it is subject to extreme seasonal contrasts as a result of its latitude (36-44°N). All these factors yield daily rainfalls of considerable spatial and temporal variability (Romero et al. 1998). Among the studies related to the Spanish Mediterranean, Summer et al. (1995) associate the distribution of significant rainfalls over the island of Mallorca with recognized dominant surface circulation types.

However, the effects of defined synoptic types on hydrology, although they have been conceptually recognized for a long time and have become apparent through numerous case studies (notably of heavy precipitations in eastern Spain; see Doswell et al. 1998), have been poorly studied for Mediterranean Spain.

Lake Banyoles (42°07’N, 2°45’E), in the eastern Catalan pre-Pyrenees, is a small multi-basin lake (surface area of 1.12 km^2) of mixed tectonic-karstic origin (Canals et al. 1990) composed of six main basins (B1- B6) (Figure 2). One of the most important aspects of the hydrological environment of Lake Banyoles is the fact that basin B1 (the largest basin) supplies around the 85% of the total incoming water by subterranean springs (at approximately 75 m of depth) and the rest is supplied by river flows entering the lake from the southeast. The tectonic constraint of the lake forces the vertical discharge of ground water flow through the bottom of the basins. In addition, the subterranean springs mix the sediments above them up to a fairly sharp interface known hereafter as the lutocline (Figures 3a and 3b). The sediment in basin B2 usually remains consolidated at the bottom, with the lutocline at a depth of approximately 44 m (Casamitjana and Roget 1993, Colomer et al. 1998). Eventually, the subterranean springs in B2 supply water to the lake at a rate comparable to B1 (in the order of 0.5 m^3/s). This is possible for high precipitation periods that recharge the aquifer which in turn increase the pressure enough for incoming water to resuspend the confined and consolidated sediment at the bottom of B2. In this case sediment migrates upward and initiates the fluidization of the confined bed sediments.

We chose then to examine the dynamics of the sediment fluidization in Lake Banyoles associated with meteorological conditions for two main reasons. First, the time evolution of sediment fluidizations in basins B1 and B2 has been recorded over the past 19 years; records show that the sediment fluidization in B1 is permanent (chronic fluidization) while in basin B2 it develops episodically (episodic fluidization). Second, the sediment fluidizations are of great limnological interest because convection occurs above the lutocline interface (Colomer et al. 2001, Colomer et al. 2003). These phenomena carry particles in suspension from lutocline upward into the lake water column which affects water quality and also both fish distribution and sedimentary records between basin B1 and B2 as reported by Serra et al. 2002 and Serra et al 2005. For both limnological and climatological reasons it is therefore important to investigate the time-series of historical observations of fluidization events in basin B2 in view of elucidating the relevant synoptic atmospheric circulations and associated rainfall affecting the limnology of the lake.

Following this introduction, the paper is organised into different sections. Both the analysis of the meteorological parameters and the observations of sediment fluidizations in basin B2 are described in the Data and Analysis section. In the Results and Discussion section we present the relationship between the sediment fluidization events and the local rainfall in the recharge area and also compare them with the atmospheric patterns predicted by the atmospheric circulation model. We finish with the Conclusions section.

Data and analysis

Classification of daily atmospheric circulation patterns

The climatological counterpart of this study is underpinned by earlier research, which derived 19 characteristic atmospheric patterns (APs) responsible for significant rainfall in Mediterranean Spain (Romero et al. 1999b). Specifically, atmospheric states of all days in the period 1984-93 in which at least 5% of the 410 rain gauge stations shown in Figure 1 registered more than 5 mm (1275 days) were classified into 19 classes using principal components analysis and cluster analysis (see the details in Romero et al. 1999b). The classification was based on the flow patterns at 925 and 500 hPa over the region shown in Figure 1 (later shown as a shaded square in Figure 10), using the gridded meteorological analyses of the European Centre for Medium-Range Weather Forecasts (ECMWF) as input data. In fact, the synoptic classification was also attempted based on grid analyses of temperature, relative humidity, horizontal wind components and other composite fields, but the most satisfactory results in terms of the relationship between the resulting atmospheric patterns and certain daily rainfall spatial distributions known for the region (Romero et al. 1999a) were obtained from a combination of the geopotential height fields at 500 and 925 hPa. This is not surprising, since these fields already contain, either explicitly or implicitly, essential information about important dynamic and thermodynamic physical processes behind precipitation generation and distribution: the dynamic forcing for vertical motion by advection of vorticity at upper levels; the presence of cold pools aloft; the sign and intensity of low tropospheric temperature advection; the interaction of low-level flow with the topography; and the moisture content of surface air masses with long paths over the Mediterranean Sea or Atlantic Ocean.

This study requires a long-term seasonal analysis of the AP frequencies and the search for anomalies in their persistence during the fluidization periods. For that purpose, daily atmospheric states during the period January 1970- August 2002 were matched against the 19 AP types described above, or as insignificant ("not rainy") situations. Input meteorological data for this long-term classification were taken from the ECMWF ERA-40 reanalysis at 12 UTC. This is a long, homogeneous, high-quality data base suitable for synoptic-scale studies like the present one (see http://data.ecmwf.int/data/ for specific information about ERA-40).

Several techniques exist for the matching of individual daily atmospheric patterns to the previously derived 19 'typical' APs. The one chosen classifies the circulation for each ERA-40 day by matching it with the closest observed day within the 1984-1993 ECMWF data sets: an analogue procedure. If the matched day within the ECMWF set was not itself classified within one of the 19 APs then the day is simply considered as a not rainy situation. Matching is performed with a similarity index (d) utilizing the Pearson product-moment correlation coefficients for the combined 925 (r_{925}) and 500 (r_{500}) hPa geopotential height fields:

$$d = \sqrt{(1 - r_{925})^2 + (1 - r_{500})^2} \qquad (1)$$

where the correlation coefficient is calculated using the field values at grid points included within the inner square shown in Figure 1 (see also Figure 10). Similar analogue approaches have been used in climate research to good effect (e.g. Summer et al. 2003). Out of the 11932 days included in the 1970-2002 period, 3953 were classified among the 19 AP classes, thus representing about one third of total days, in close agreement with the observed percentage of significant rainy days in Mediterranean Spain (Romero et al. 1998).

Historical observations of sediment fluidizations in basin B2

The fluidization events (F1, F2, etc) were detected by measuring the depth of the lutocline Z_L in basin B2. The lutocline level was well detected by seismic profiles (Figure 3a and 3b), echo sounding profiles or continuous water temperature measurements. In the third case, measurements of water temperature in the water column of B2 showed that the temperature at and below the lutocline in B2 changed from around 17.5°C at the beginning of the fluidization process to 19.1°C in the fluidized state. For all registered values at the lutocline depth an inverse temperature gradient of 2-8°C/m was found. The mean sediment concentration below the lutocline in both B1 and B2 depends on the state of fluidization, and varied between 100 and 280 g/l, therefore in both the seismic and echo sounding profiles the lutocline appeared in the plots as a flat line (Figure 3). As shown in the south to north seismic transect in Figure 3, B1 presented an active fluidization with the lutocline located at a depth of 24 m while the sediment in B2 was confined at the bottom (non-fluidized state) with the lutocline located at a depth of 44 m.

In the last nineteen years (1986-2004), while the sediments in B1 were found to be always in suspension (termed here as chronic fluidization), the sediments in B2 presented high temporal variability depending on the fluidization events (Figure 4). Two sparse cases (F1 and F2) in 1976-1977 and cases from F3 to F11 in the period of continuous measurements (1986-2004) have been detected out of 11 vertical migrations of the lutocline in basin B2. The strength of a fluidization event was quantified by the maximum vertical migration of the lutocline. Based on this, the largest migration was detected during the F7 event in 1996-1997, when the lutocline in B2 migrated to a depth of about 20.5 m. (The maximum vertical migration of the lutocline from the historical record is about 24 m.) Of remarkable interest is the fact that the major fluidization events may last more than one year, especially because some events are coupled: F3-F4, F5-F6, F7-F8 and F10-F11. This behavior can be explained by taking into account that a second fluidization is quite possible after one fluidization although the inflow of water is not so high. Also, the fluidization in B2 does not happen each year, so it has not been related to seasonal dynamics. The fluidizations, therefore, happened eventually or episodically without following any periodic evolution. For all of the above reasons, the fluidization events in B2 have been termed as episodic.

The relationship between the timing of sediment fluidization events and local monthly rainfall was investigated using daily data from the nearest meteorological stations at Castelló d'Empúries, Jafre, Les Planes d'Hostoles, Banyoles and Darnius. The first three are located ~30 km from the area of aquifer recharge, while Banyoles is ~19 km away and Darnius is at a distance of ~15 km. The rainfall in the Darnius meteorological station has therefore been chosen as characteristic of the rainfall of the area of aquifer recharge.

Results and discussion

Sediment fluidization events related to local rainfall

The mean monthly rainfall in Lake Banyoles (available period: 1984-2004) and in the area of the aquifer recharge (available period: 1987-2004) are shown in Figure 5. On average, monthly rainfalls present marked seasonal variation, with maximum values concentrated in spring and autumn for both meteorological stations. The rainfall in both areas is explained by different circulation patterns: a) large depressions lying above western Spain, which provide southwesterly-westerly flows and also warm and moistened southerly flows over the Pyrenees mountains, a pattern essentially linked to the Atlantic dynamics which quasiperiodically influences the Spanish latitudes during the cold season; and b) southerly-southeasterly onshore flows, cold fronts from the north, and also easterly to northerly flows induced by frequent depressions in the north of the Mediterranean basin, a circulation contributed by Atlantic disturbances circulating at higher latitudes, and also influenced by secondary cyclones generated frequently over the northern part of the Mediterranean basin. The accentuated maximum in October is related to synoptic disturbances that become very effective through the strong interaction between large amounts of water vapor released from the warm Mediterranean and coastal terrain features (Romero et al. 1999b, Doswell et al 1998). The relative maximum in December is associated with rainfall related to the passage of cold fronts over the Iberian Peninsula, associated with mid-latitude disturbances and mainly affecting the very north of Catalonia, including the area of aquifer recharge.

The local rainfall in the area of aquifer recharge during the months of the initiation of the sediment fluidizations in basin B2 of the lake is shown in Figure 6, where the central bar (from the 5 bars in each fluidization) coincides with the month of the initiation of the process. The term initiation of the fluidization refers to the first day on which the vertical displacement of the lutocline was observed. It should be borne in mind here that the frequency of measurements is likely to limit the representativeness of data. Depending on the type of measurements, a maximum of a week is waited between a day of heavy rainfall and measures of lutocline depth. Despite this reservation, however, initiation of the fluidization usually coincides with the maximum mean monthly rainfall in Figure 6, which was about 250-350 mm (F2, F3, F7, F9 and F10). For the fluidizations following a previous one (F4, F6, F8 and F11), a monthly local rainfall of about 200 mm is enough to drive the next event in B2. As shown in both plots in Figure 7, the anomaly of rainfall defined as the difference between the local monthly and the mean local monthly rainfall (for the whole period of available data) divided by the last one present the largest values (of about 100-300 %) during the fluidization events. A value of 200% means that the value of the local monthly rainfall is three times the mean monthly rainfall. The mean anomalies of rainfall in the area of aquifer recharge and in Lake Banyoles, for the months of the initiation of the fluidization events, are 167 and 151 %, respectively. Then, the local monthly rainfalls are 2.67 and 2.51 times the mean monthly rainfall, respectively.

It is worth noting that the extent and duration of a fluidization event not only depends on the local monthly rainfall of a particular month but on the cumulative monthly rainfall in the months proceeding and after the initiation of the process. Fluidization F9 presents an extreme behavior, in that the maximum local monthly precipitation value ever recorded in the area of aquifer recharge (April 2002) drove this fluidization, although with a weak vertical extent and duration, of about 6 m and 4 months, respectively (Figure 4). This fluidization was preceded by a very dry period on the whole, and therefore the sediment could not be maintained in suspension and lutocline migrated down. On the contrary, F6 lasted for about 16 months (June 1992 to October 1993) as a result of large sustained precipitation in the area of aquifer recharge. Based on this interpretation, another variable comes into question as a possibly useful empirical determinant of the extent of a fluidization event: the accumulated monthly rainfall in the months preceding the event. Thus, we can make the assumption that the extent and duration of a fluidization event is associated with monthly rainfall accumulated over some fixed period of time; i.e. that the vertical migration of the lutocline is correlated with the monthly anomalies of local rainfall in the area of aquifer recharge, $P_{J,N}$, defined in discrete form as

$$P_{J,N} = \frac{1}{N} \sum_{j=J-N+1}^{j=J} P_{j,N} \qquad (2)$$

where the location parameter J is the month of the year on which the fluidization process begins, the integrating parameter N is the number of preceding months over which the sum is performed, and $P_{j,N}$ is the monthly rainfall in month j. The best linear relationship between the vertical depth of the lutocline and $P_{J,N}$ is then obtained by finding the values of N that maximize r^2, the proportion of variance explained (Livingstone 1997, Livingstone 1999). Values of r^2 were computed at monthly intervals of $3 \leq N \leq 12$, which included seasonal and annual accumulated rainfall. The maximum explained variance (r^2 = 50.6 %) was obtained with the monthly rainfall accumulated for the previous 10 months (Figure 8). The mean duration of all fluidization events is 10.1 months, which is also in accordance with the mentioned relationship. The result reflects the fact that the tendency in the accumulated rainfall during the previous 10 months determines whether the fluidization will happen or not. In cases where the bed is already fluidized, the rainfall behavior for the previous 10 months will determine its time evolution.

It is interesting to remark that the maximum distance the lutocline migrated was about 24-22 m. This maximum excursion is limited by the fact that vertical velocity of incoming water diminishes from the inflow at the basin entry (at 85 m of depth) up to the lutocline depth (because of increasing transversal area), and at this depth the downward settling vertical velocity of the sediment suspension equals the upward vertical velocity of water (Colomer et al. 2001). Another possible explanation of the limited maximum excursion of lutocline is the fact that the sediment suspension flowed out the basin because at the south of Basin B2 the depth is about 20-22 m; this process would only take place during the major fluidization events F6, F7, F8 and F11. Finally, for the coupled fluidizations, the input of water in the aquifer increased its pressure and, as a result, the water entering into an already fluidized bed could produce a secondary migration of the lutocline that reached upper distances, i.e. less depth if counting from the water surface, as in the F3-F4 and F10-F11 cases.

Out of the 11 fluidization processes, 7 took pace in the expected seasons of maximum rainfall: spring and autumn (as shown in Fig. 5), 3 cases: F5, F7 and F8 took place in winter, as a direct result of the local monthly rainfall of December, and only F6 initiated a fluidization in the warm season of summer (June 1992). All in all, in the period 1986-2004, the sediment bed in B2 remained in suspension in 39.9% of the whole historical record, defining its episodic behavior.

Based on the above timing of initiation and duration of fluidizations, a major limnological implication comes into question: fluidizations F1, F3, F5, F7, F8, F10 and F11 in Lake Banyoles either initiated or initially developed when the water column of the lake was mixed; the mixing period of the lake was established between the end of October and mid-April and the rest of time the water column of the lake was stratified. In addition, Colomer et al. (2001) found the lutocline to be warmer (because water entry at the bottom of the basins is 19.1 °C, as mentioned previously) than the water above the lutocline. The difference in temperature between the suspension zone and the water above induces the development of a turbulent convective plume above the lutocline. As a major characteristic of convection from an isolated source, the plume entrains particles from the lutocline and carries upward a suspension of clay and silt particles with particle volume concentrations of ~ 5-10 μl L^{-1}. Because of the temperature inversion at the lutocline, the plume is negatively buoyant. As a result, it develops upward and in the absence of a thermal stratification background or in the presence of a weak one (as it is in the mixed lake period) it is expected to reach the surface waters after which it spreads laterally, with the consequent change of water quality in terms of an increase of the suspended particle concentration. It can be expected, then, that the suspended particles change the clarity of the water, which might imply a habitat constraint for fishes as limiting their feeding opportunities and other visual activities (Moyle and Cech 1996, Mathews 1998, Garcia-Berthou 1999, Serra et al 2002). Not only this, as Casamitjana and Roget (1990) found, but whenever the water column in B2 is stratified and the sediment compacted at the bottom of the basin (no inflow), at the top (22 m of depth) of the basin, a secondary, stationary thermocline develops; it is only destroyed in the cold months of January and February. Then, during the major fluidizations events, as lutocline migrates upward, the secondary thermocline is eroded and finally vanishes, and as a result the lake hypolimnion warms up not only because of the heat released by the lutocline in B1 but because of the lutocline in B2, which is in the order of ~ 50 to 200 Wm^{-2} each (Casamitjana and Roget 1988).

Sediment fluidization events related to Atmospheric Patterns

The classification of daily atmospheric circulations for the period 1970-2002 described in the previous section allowed the daily rainfalls in the area of study to be associated with one of the 19 emergent APs. The APs may be compared with each other in terms of both 500 and 925 hPa circulation dissimilarities within the considered geographical window. In some cases, the structures at 500 hPa, which are smoother, are relatively similar but the surface circulations exhibit substantial differences. In other cases, both levels show very similar aspects in some areas, but in other areas important differences in the position, orientation, size or depth of the disturbance appear (Romero et al. 1999b). In this section, though, only the most frequent atmospheric patterns during the months of onset of the fluidization events (comprising a total of 525 days) are studied in detail. Here we consider an atmospheric pattern to be relevant if its frequency is larger than 5%. Accordingly, the atmospheric patterns AP3, AP4, AP8, AP9, AP14 and AP19 were identified as the most frequent at the time of initiation of the fluidization events (Figure 9): AP8 (18%), AP19 (12%), AP14 (11%), AP3 (9%), AP4 (7%) and AP9 (7%) account for a total of 64% of all days. These atmospheric patterns are shown in Figure 10 and will be discussed in detail.

Also, for the whole 1970-2002(August) data set, the monthly incidence of the derived atmospheric patterns (AP1 to AP19) is quantified by introducing the so-called month-frequency ratio ($AP_{ijmonth\text{-}frequency}$). It is defined, for each month and AP, as the ratio between the number of days with the selected AP to the total number of days presenting any AP, using the whole period of data (Figure 11) without considering the non rainy days (with AP = 0), as follows:

$$AP_{ijmonth-frequency} = \frac{N(AP_{ij})}{\sum_{i=1}^{i=19} N(AP_{ij})} \tag{3}$$

where $N(AP_{ij})$ is the number of days with an AP in the month j. This index is useful to assess the monthly AP climatology in the Spanish Mediterranean area for the 33-year period, i.e. to determine to which degree each AP is expected in any given month on rainy days.

Pattern AP3 (Figure 10) is characterized by deep depressions centered to the northwest of the Iberian Peninsula. At upper levels, the nearly meridionally oriented transverse axis implies a general southwesterly flux and advection of positive vorticity over the whole of the Mediterranean region of Spain. In the eastern part of the region, there is warm and humid advection from the south-southeast, favoring rainfall development over the exposed areas of eastern Spain, including Catalonia. Pattern AP3, comparatively frequent during fluidization episodes (9%, Figure 9), exhibits its maximum occurrence during autumn, especially in October (10.6%) and November (10.8%). These values are above the values during spring and winter (Figure 11). Pattern AP3 mainly developed in fluidizations F3 and F5.

Circulation AP4 (Figure 10) presents a frequency of 7 % (Figure 9) during fluidization periods and represents southwesterly flows at all levels associated with low pressure systems to the northwest of Spain. Characteristically, the geopotential fields indicate the presence of weak cold fronts moving into the Iberian Peninsula from the west. Apart from the Atlantic rainfall patterns that affect the west of Catalonia, rainfall in the area of study is also favored. This circulation presents almost equal month-frequencies in August, October and December (Figure 11), and seasonally it presents the highest frequency in winter and autumn. It showed high occurrence in fluidization F1, F7 and F8.

The most persistent circulation during the onset of the fluidization events, AP8 (Figure 10, 18%), presents occasions when short baroclinic waves occur over the Iberian Peninsula. The general circulation is characterized by deep troughs in the westerlies at upper levels lying over western Spain, but no appreciable tilting. At the surface, the northwesterly winds are associated with the passage of cold fronts. Rainfalls in Catalonia are largely activated by this pattern since that area is affected by maximum positive vorticity advection at 500 hPa. In addition, moisture from the Mediterranean is available ahead of the cold front. AP8 tends to appear in summer (June and July), followed in frequency by spring (April and May). It developed mainly during fluidizations F6, F9 and episodically in F5 (December 1991). However, this atmospheric pattern is not considered frequent for that month of the year (Figure 11).

The AP9 composite (Figure 10) basically represents west to northwesterly winds at all levels following the passage of cold fronts from the Atlantic to the Mediterranean. This appears to be an ideal situation for the development of orographically enhanced rainfalls in the South Mediterranean. The northeastern regions (Catalonia and the Balearic Islands) are close to the cold front and this is reflected in the typical rainfalls of winter and spring, where it presents large month-frequencies (Figure 11). It showed high occurrence in fluidization F2.

AP14 (Figure 10), with an 11% frequency during the months of the initiation of the fluidizations, is characterized at 500 hPa by an accentuated trough with a positively tilted axis which is restricted to the central part of the Iberian Peninsula. The area with maximum advection of vorticity is the southeast and east, which also benefits from rainfall generated by the warm and humid Mediterranean flows induced by the surface pressure distribution. Rainfalls in the interior of Andalusia, which is the nearest zone to the centre of the disturbance and receives favorable northwesterly surface winds, are also produced. Rainfall also occurs in the exposed Pyrenees. This circulation pattern exhibits its maximum month-frequency in the months of summer and spring (Figure 11), and the 925 hPa geopotential fields indicates relatively low pressure areas over the Iberian and African plateau, a signature of warm-season thermal lows. This circulation was episodically present in fluidizations F2, F4 and F9. It should be remarked that in April 2002, in the area of aquifer recharge, it rained 324.5 mm (the largest value registered for the whole period of analysis), and is therefore associated with the F9 event.

Finally, cluster AP19 (Figure 10) comprises 500 hPa lows over the Gulf of Lyon with associated low-level cyclone to the east of the Balearic Islands, which may drive strong rainfall in the north-east of Catalonia. This circulation pattern exhibits high frequency during fluidization periods (12%, Figure 9) and is more frequent in the months of spring and winter (Figure 11) than in autumn. It showed high occurrence in fluidizations F2 and F5.

Also, we can define the $AP_{ij\text{-frequency}}$ (complementary to the previous month-frequency). It is defined as the ratio between the number of days in a month with one AP to the number of total days with the same AP during the whole period studied, as follows:

$$AP_{ij-frequency} = \frac{N(AP_{ij})}{\sum_{j=1}^{j=12} N(AP_{ij})} \tag{4}$$

where $N(AP_{ij})$ is the number of days with an AP, for i=1 to i=19, in a month. This frequency gives information about the most relevant months or seasons (the sum of 3 months) for each AP; this data is summarized in Table I where the $AP_{ij\text{-frequency}}$ for each season (winter, spring , summer and autumn) for the whole period of analysis (1970-2002) are presented. The Atlantic type circulations AP3 and AP4 (associated with fluidizations F1, F3 and F7) show similar frequencies in winter, spring and autumn; and AP9 shows an accentuated maximum in winter followed by spring. The Mediterranean type circulation AP19 showed its maximum in spring and winter, while AP8 and AP14 presented maximum values in spring and summer (minimum in winter).

When the incidence of the atmospheric circulation patterns during fluidization events is compared against their total incidence, the results can be summarized by the fact that the derived APs for all days belonging to the months of initiation of the fluidization events (a total of 525 days) exhibit large positive anomalies, 84.2% and 83.1%, respectively, compared to the monthly-frequency (Eq. 3) and AP-frequency (Eq. 4) derived for the whole set of days. Finally, even though these statistics give information on AP climatology, the type of rainfall episodes associated with the fluidization events under the responsible circulation patterns is not immediately clear. This is briefly discussed in next section.

Atmospheric patterns and torrential rainfalls

Two types of rainfall episodes are found to act as precursors of fluidizations: (a) moderate to heavy rainfalls occurring in a few days, possibly with torrential character on some days (i.e. greater than 50 mm in 24 h), as in fluidizations F2, F3, F5, F6, F7, F9, F10 and F11, and (b) light to moderate rainfall, but extending –intermittently– over a long enough period (months), as in F1, F4 and F8. A total of 36 torrential rainfalls measured in the period of sediment fluidizations were associated with the most frequent atmospheric patterns AP3, AP4, AP8, AP9, AP14 and AP19. As seen in Figure 12, the six atmospheric patterns present a total of 61.1% of the total number of days with torrential rainfalls. It is noteworthy that AP13, although not very frequent during the fluidization episodes (recall Figure 9), explains a significant fraction of the torrential rainfall registered during the fluidizations (Figure 12). It seems then that AP13 strongly contributed to the rain in the area of study during very few days. This circulation (not shown) represents the presence of large and intense cut-off cyclones over the southern part of the domain, above the Strait of Gibraltar (Figure 1). The associated surface circulation imposes a general easterly regime over the domain, with a continuous supply of moisture towards the Mediterranean coast. Considering all of Mediterranean Spain, AP13 is the atmospheric circulation pattern with the highest propensity towards heavy rain (as much as 38% of AP13 days are torrential). In contrast, the more frequent AP9 pattern for the fluidization phenomenology (Figure 9) exhibits a very low propensity towards heavy rainfalls, both in the study zone (Figure 12) and for the bulk of Mediterranean Spain (less than 4% of AP9 days are torrential somewhere in the area).

Previous studies by Romero et al. (1999b) associated torrential rainfall in Mediterranean Spain with atmospheric circulation; they found that in relation to the total rainy days, torrential days have an incidence under situations AP3 and AP14 exceeding 20%, mainly over western Andalusia and eastern Spain, respectively, rather than in the study zone. They also found a certain incidence of torrential rainfall towards the study zone for atmospheric patterns AP13 and AP19, which appears to be consistent with the results shown in Figure 12. All these circulations are characterized in the middle troposphere by closed cyclonic circulations or very accentuated shortwave troughs extending towards the south of the domain. At low levels, they exhibit a significant level of warm advection towards some areas of Mediterranean Spain, particularly Catalonia, except AP19 which is characterized by northerly flows and thus cold advection. Previous studies (Romero et al. 1998, 1999a) also found the preference of heavy precipitations in coastal areas and interior mountainous zones, which is the case in the area of study because of its proximity to the Pyrenees ranges. This scenario has a specific importance in the autumn season, as synoptic disturbances become very effective through the strong interaction between large amounts of water vapor released from the warm Mediterranean and coastal terrain.

Conclusions

This study presents data on sediment fluidization events in Lake Banyoles and their relationship with accumulated rainfall in the recharge area. The characteristic rainfall atmospheric patterns over the studied area have been analyzed. Among the 19 circulation types some atmospheric patterns, the Atlantic types: AP3, AP4 and AP9, and the Mediterranean types: AP8, AP14 and AP19, have been found to be responsible for the large or torrential rainfall over the recharged area and associated to the sediment fluidization events in the lake. AP13 has also been found to explain a significant fraction of the torrential rainfall. Out of the 11 fluidization processes, 7 took place in the expected seasons of maximum rainfall: spring and autumn, 3 cases (F5, F7 and F8) took place in winter, as a direct result of the local monthly rainfall of December, and only F6 initiated a fluidization in the warm summer season. Two types of rainfall episodes are found to act as precursors of fluidizations: (a) moderate to heavy rainfalls occurring in a few days, possibly with torrential character on some days, as in fluidizations F2, F3, F5, F6, F7, F9, F10 and F11, and (b) light to moderate rainfall, but extending –intermittently– over a long enough period (months), as in F1, F4 and F8.

It has been found that the lutocline migrated a maximum distance of about 24-22m while for one case, F9, the lutocline migration was shorter than in the other cases, probably due to the fact that fluidization occurred after a large dry period which could have produced a decrease in the water level of the aquifer recharge. The large excursion observed in the major set of fluidization (F6, F7, F8 and F11) is limited by the fact that vertical velocity of incoming water diminishes from the inflow at the basin entry (at 85 m of depth) up to the lutocline depth. In all probability, the maximum excursion of lutocline is, in fact, limited by the bathymetry of the basin surround which made the sediment suspension flow out the basin because at the south of Basin B2 the depth is about 20-22 m. Finally, for the coupled fluidizations, the input of water in the aquifer increased its pressure and, as a result, the water entering into an already fluidized bed could produce a secondary migration of the lutocline that reached upper distances, i.e. less depth if measuring from the water surface, as in the F3-F4 and F10-F11 cases. All in all, the major fluidization events described herein produce large charges in the hypolimnetic waters of the Lake Banyoles because of the heat associated with the incoming warm waters, which , in turn, affect the whole column structure of the lake, specially in the mixing period.

References

Blenckner, T., and D.L. Chen. 2003. Comparison of the impact of regional and North Atlantic atmospheric circulation on an aquatic ecosystem. Climate Research **23 (2):** 131-136.

Bonell, M., and G. Summer. 1992. Atmospheric circulation and daily precipitation in Wales. Theor. Appl. Climatol. **46:** 3-25.

Canals, M., Got, H., Julia, R., and J. Serra. 1990. Solution-collapse depressions and suspensates in the limnocrenic lake of Banyoles (NE Spain). Earth Surf. Proc. Land. **15:** 243-254.

Casamitjana, X., Roget, E., Jou, D., and J.E. Llebot. 1988. Effect of suspended sediment on the heating of lake Banyoles. Journal of Geophysical Research **93 (C8):** 9332-9336.

Casamitjana, X., and E. Roget. 1990. The thermal structure of Lake Banyoles. Verh. Internat. Verein. Limnol. **24:** 88-91.

Casamitjana, X., and E. Roget. 1993. Resuspension of sediment by focused groundwater in Lake Banyoles. Limnology and Oceanography **38(3):** 643-656.

Colomer, J., Ross, J.A. and X. Casamitjana. 1998. Sediment entrainment in karst basins. Aquat. Sci. **60:** 338-358.

Colomer, J., Serra, T., Piera, J., Roget, E., and X. Casamitjana. 2001. Observations of a hydrothermal plume in a karstic lake. Limnol Oceanogr. **46:** 197-203.

Colomer, J., Serra, T., Soler, M., and X. Casamitjana. 2003. Hydrothermal plumes trapped by thermal stratification. Geophys. Res. Lett. 30, 21, 2092, [doi:10.1029/2003GL018131]

Doswell III, C.A., Ramis, C., Romero, R., and S. Alonso. 1998. A diagnostic study of three heavy precipitation episodes in the western Mediterranean regions. Weather Forecasting **13:** 102-124.

Garcia-Berthou E. 1999. Spatial heterogeneity in roach (Rutilus rutilis) diet among contrasting basins within a lake. Arch. Hydrobiol. **1456:** 239-256.

George, D.G., Maberly, S.C., and D.P. Hewitt. 2004. The influence of the North Atlantic Oscillation on the physical, chemical and biological characteristics of four lakes in the English Lake District. Freshwater Biology **49(6):** 760-774.

Gerten, D., and R. Adrian. 2000. Climate-driven changes in spring plankton dynamics and the sensitivity of shallow polymictic lakes to the North Atlantic Oscillation. Limnology and Oceanography **45(5):** 1058-1066.

Gerten, D., and R. Adrian. 2001. Differences in the persistency of the North Atlantic Oscillation signal among lakes. Limnology and Oceanography **46(2):** 448-455.

Livingstone, D.M. 1997. Break-up dates of Alpine lakes as proxy data for local and regional mean surface air temperatures. Climate Change **37:** 407-439.

Livingstone, D.M. 1999. Ice break-up on southern Lake Baikal and its relationship to local and regional air temperatures in Siberia and to North Atlantic Oscillation. Limnology and Oceanography **44 (6):** 1486-1497.

Mathews, W.J. 1998. Patterns in freshwater fish ecology. Chapman and Hall.

Martin E., Timal, B., and E. Brun. 1997. Downscaling of general circulation model outputs: simulations of the snow climatology of the French Alps and sensitivity to climate change. Climate Dynamics **13:** 45-56.

Moyle, P.B. and J.J. Cech, Jr. 1996. Fishes: An introduction to ichthyology. Prentice Hall.

Omstedt, A. and D.L. Chen. 2001. Influence of atmospheric circulation on the maximum ice extent in the Baltic Sea. Journal of Geophysical Research (Oceans) **106 (C3):** 4493-4500.

Romero, R., Guijarro, J.A., Ramis, C., and S. Alonso. 1998. A 30 year (1964-1993) daily rainfall data base for the Spanish Mediterranean regions: first exploratory study. International Journal of Climatology **18:** 541-560.

Romero, R., Ramis, C., and J.A. Guijarro. 1999a. Daily rainfall patterns in the Spanish Mediterranean area: an objective classification. International Journal of Climatology **19:** 95-112.

Romero, R., Summer, G., Ramis, C., and A. Genovés. 1999b. A classification of the atmospheric circulation patterns producing significant daily rainfall in the Spanish Mediterranean area. International Journal of Climatology **19:** 765-785.

Serra, T., Colomer, J., Zamora, Ll., Moreno-Amich, R., and X. Casamitjana. 2002. Seasonal development of a turbid hydrothermal plume in a lake. Water Research **36(11):** 2753-2760.

Serra, T., Colomer, J., Julià, R., Soler, M. and X. Casamitjana. 2005. Hydrothermal dynamics dominating sedimentary records in lake Banyoles. Sedimentology (in press).

Summer, G., Guijarro, J.A., and C. Ramis.1995. The impact of surface circulations on the daily rainfall over Mallorca. International Journal of Climatology **15:** 673-696.

Summer, G.N., Romero, R., Homar, V., Ramis, C., Alonso, S., and E. Zorita. 2003. An estimate of the effects of climate change on the rainfall of Mediterranean Spain by the late twenty first century. Climate Dynamics **20:** 789-805.

Weyhenmeyer, G.A., Blenckner, T., and K. Pettersson. 1999. Changes of the plankton spring outburst related to the North Atlantic Oscillation. Limnology and Oceanography **44(7):** 1788-1792.

Yarnal, B. 1993. Synoptic Climatology in Environmental Analysis. Belhaven Press.

Figure Legends

Figure 1. The Spanish Mediterranean area, which comprises the regions of Catalonia, Valencia, Murcia, Andalusia, and Balearic Islands. It includes a smoothed version of its orography, the position of the rain gauge stations (410 in total), and some geographical references mentioned in the text. The two stations adjacent to Ibiza belong to the small island of Formentera, which is not represented.

Figure 2. Aerial photograph of Lake Banyoles with marked transects of measurements. The lake is divided into six basins. Basin B1 is located in the southern lobe, basin B2 in the central lobe and B3, B4, B5 and B6 in the northern lobe, some of them clearly seen in the photograph (kindly provided by the Institut Cartogràfic de Catalunya). Also in the plot, contour depths (with characteristic values in meters) are shown.

Figure 3. (a) South-North seismic transect and (b) schematic interpretation of the section from B2 to B1 (Canals et al. 1990); the lutocline is well detected by the seismic profile and is located at a depth Z_L from the surface.

Figure 4. Lutocline depth, at B2 (as shown in 3b) during the period 1986-2004, where fluidization events are identified (from F3 to F11).

Figure 5. Monthly rainfall in the area of the aquifer recharge (Darnius), black circles, and in the area of study (Banyoles), white circles, for the whole period of analysis.

Figure 6. Local monthly rainfall during the fluidization events in the area of aquifer recharge. The central value corresponds to the month of initiation of each fluidization event.

Figure 7. (a) Calculated monthly rainfall anomaly in the area of aquifer recharge (Darnius) and (b) in the area of study (Banyoles).

Figure 8. Coefficient of determination (r^2) between the vertical depth of the lutocline and the accumulated rainfall in the area of study on accumulating month N. Significance level ($P<0.01$) is shown as horizontal dotted line.

Figure 9. Percentage frequency of each AP during the period of initiation of the fluidization events.

Figure 10. Composites of the 6 most frequent APs during fluidization events. The continuous lines represent the geopotential height field at 925 hPa (contour interval, 10 m), and the dashed line represents it at 500 hPa (contour interval, 20 m). The interior rectangle represents the geographical window used for the pattern classification.

Figure 11. Month-frequencies (see text) for the 6 most frequent APs during fluidization events. The shaded rectangle represents the geographical window used for the pattern classification.

Figure 12. Percentage frequency of torrential days during the time of initiation of the fluidization events as a function of atmospheric pattern.

Table Legends

Table I. AP-frequencies (see text) for all APs, grouped by seasons.

Winter	Spring	Summer	Autumn	AP
42.5	27.5	5.2	24.8	1
53.4	19.9	1.7	25.0	2
29.5	30.5	6.2	33.8	3
32.8	27.8	11.7	27.8	4
27.8	28.6	10.5	33.1	5
26.9	32.5	10.8	29.7	6
23.8	31.0	19.7	25.5	7
14.8	37.9	28.8	18.5	8
40.1	33.2	4.7	22.0	9
39.5	20.9	2.3	37.2	10
3.3	24.2	60.1	12.4	11
32.4	29.7	2.7	35.1	12
40.8	22.4	4.6	32.2	13
9.3	35.8	33.8	21.2	14
24.5	32.7	20.4	22.4	15
11.9	28.6	34.6	24.9	16
34.2	20.8	14.2	30.8	17
31.3	31.9	12.4	24.5	18
35.0	36.0	6.6	22.4	19

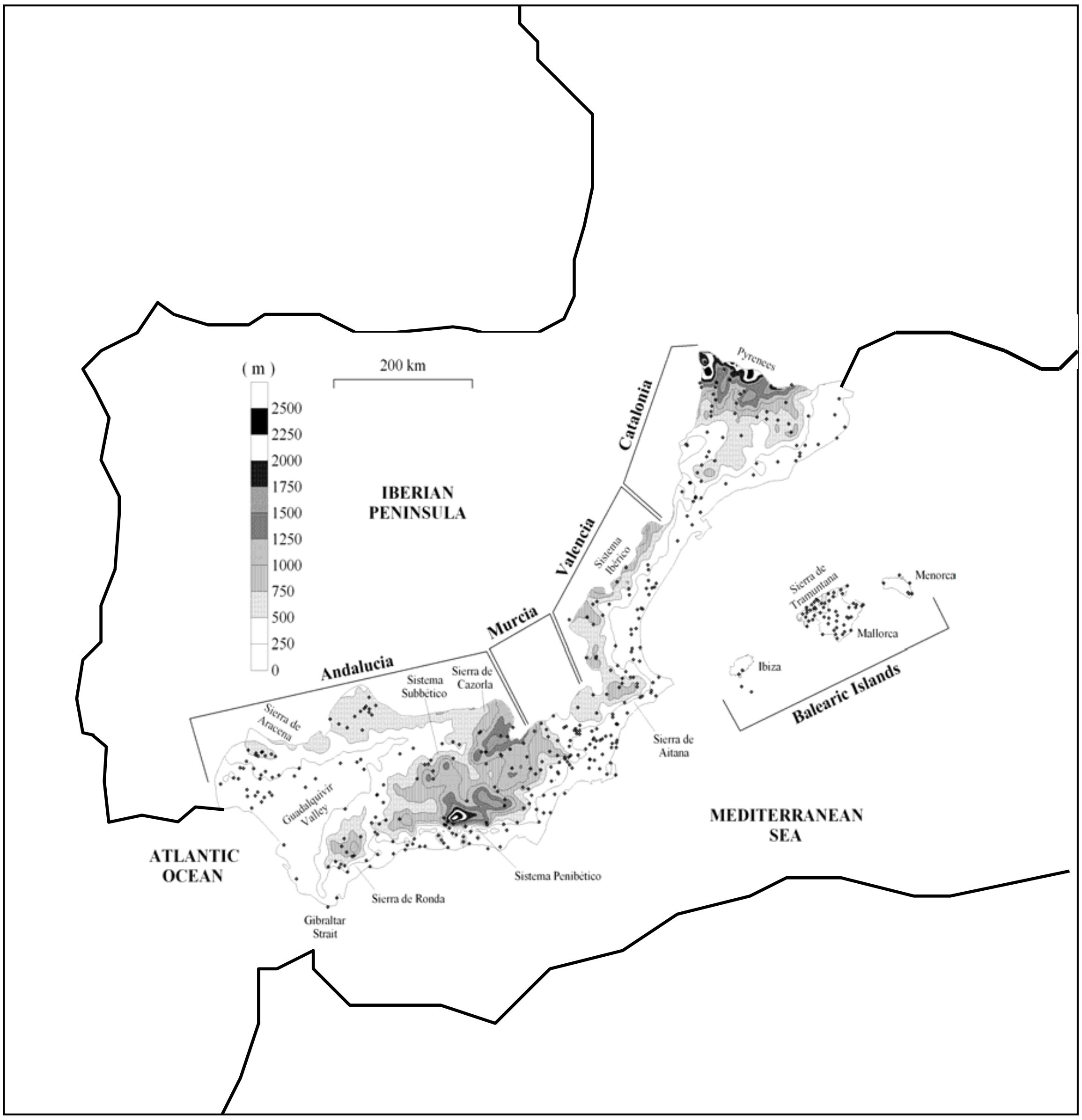
(m)
2500
2250
2000
1750
1500
1250
1000
750
500
250
0
200 km
IBERIAN PENINSULA
Catalonia
Pyrenees
Valencia
Sistema Ibérico
Murcia
Andalucia
Sierra de Aracena
Guadalquivir Valley
Sistema Subbético
Sierra de Cazorla
Sierra de Aitana
Sistema Penibético
Sierra de Ronda
Gibraltar Strait
ATLANTIC OCEAN
MEDITERRANEAN SEA
Sierra de Tramuntana
Menorca
Mallorca
Ibiza
Balearic Islands

Figure 1

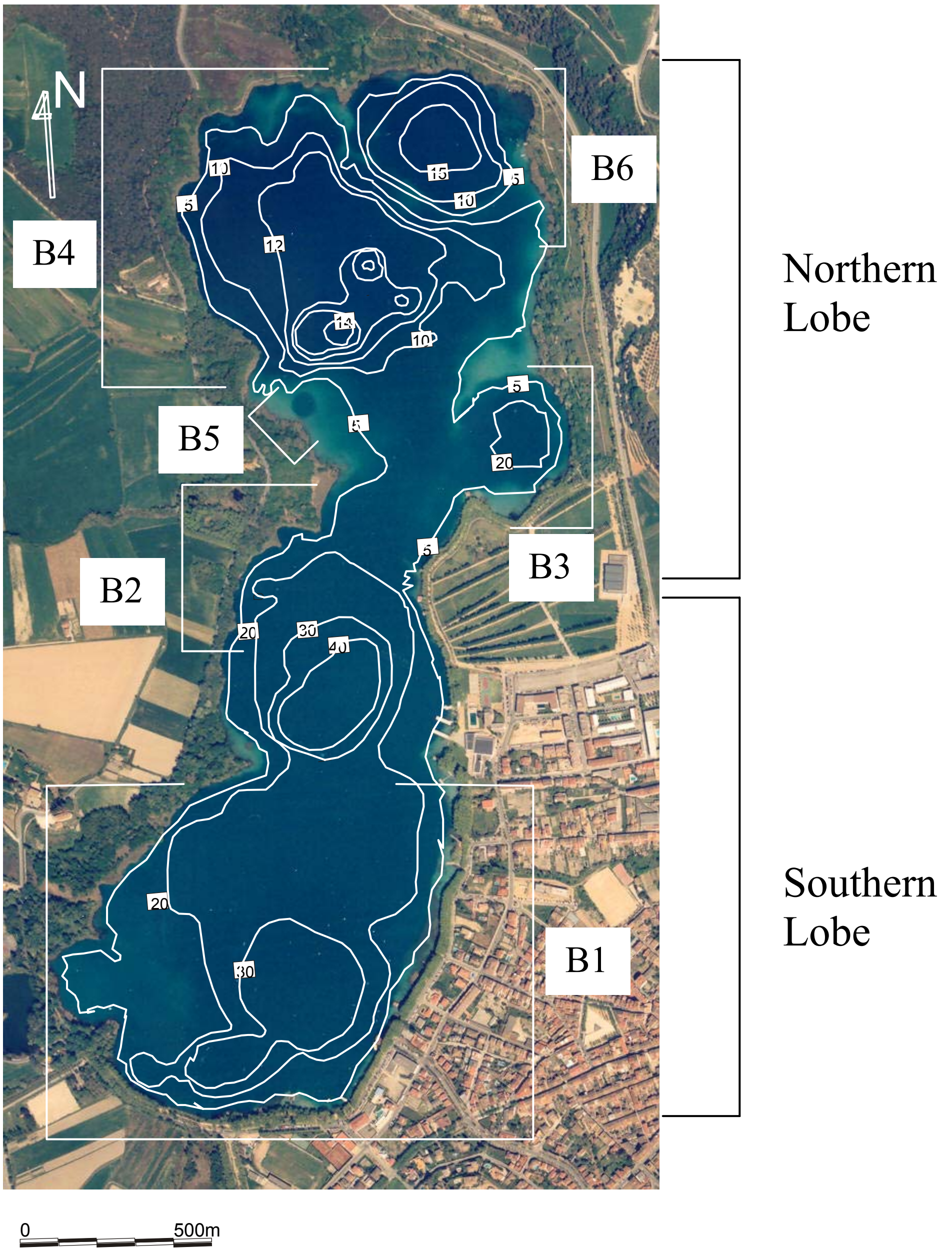

Figure 2

a

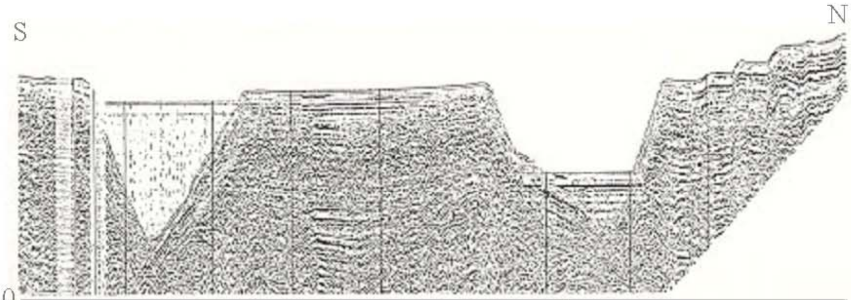

b

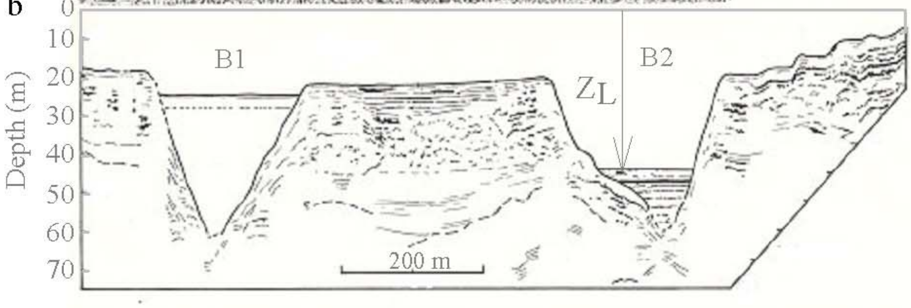

Figure 3

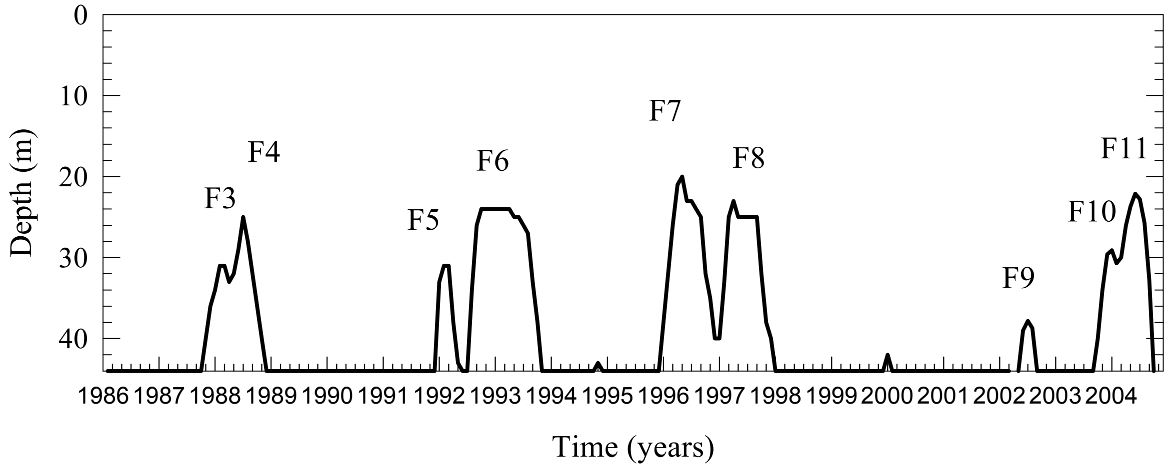

F3
F4
F5
F6
F7
F8
F9
F10
F11
0
10
20
30
40
Depth (m)
1986 1987 1988 1989 1990 1991 1992 1993 1994 1995 1996 1997 1998 1999 2000 2001 2002 2003 2004
Time (years)

Figure 4

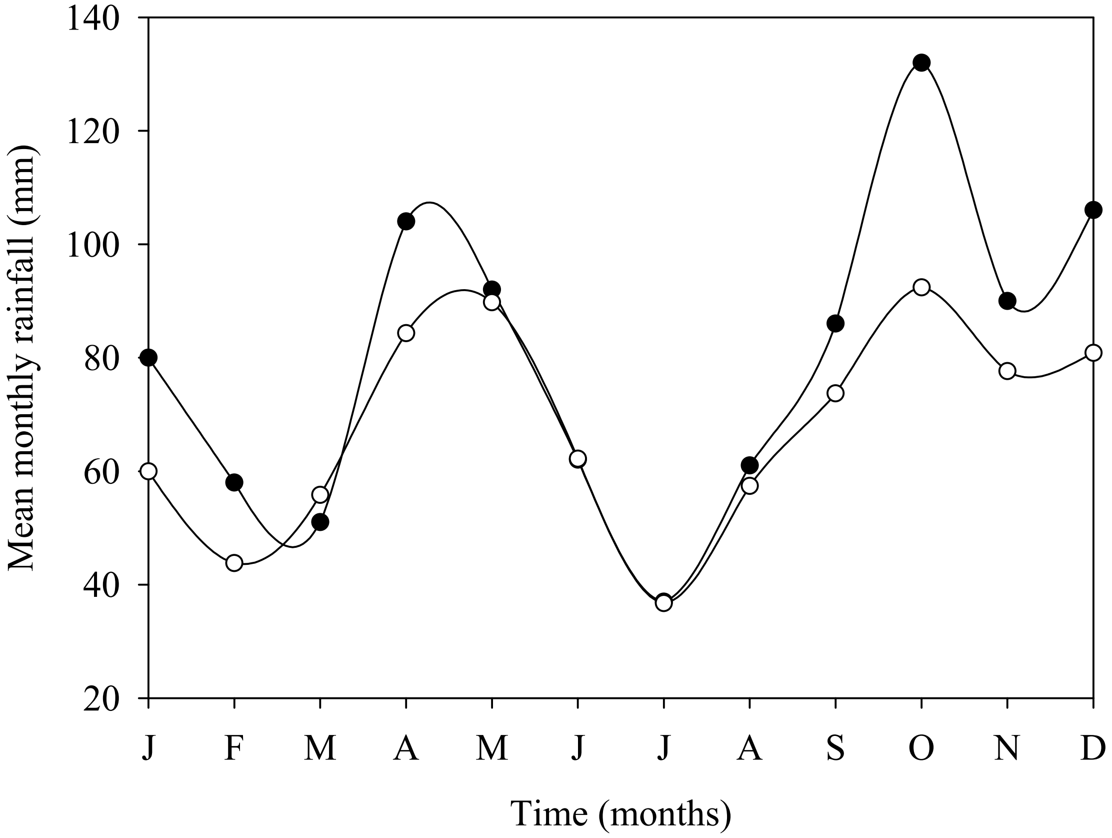
140
120
100
80
60
40
20
Mean monthly rainfall (mm)
J F M A M J J A S O N D
Time (months)

Figure 5

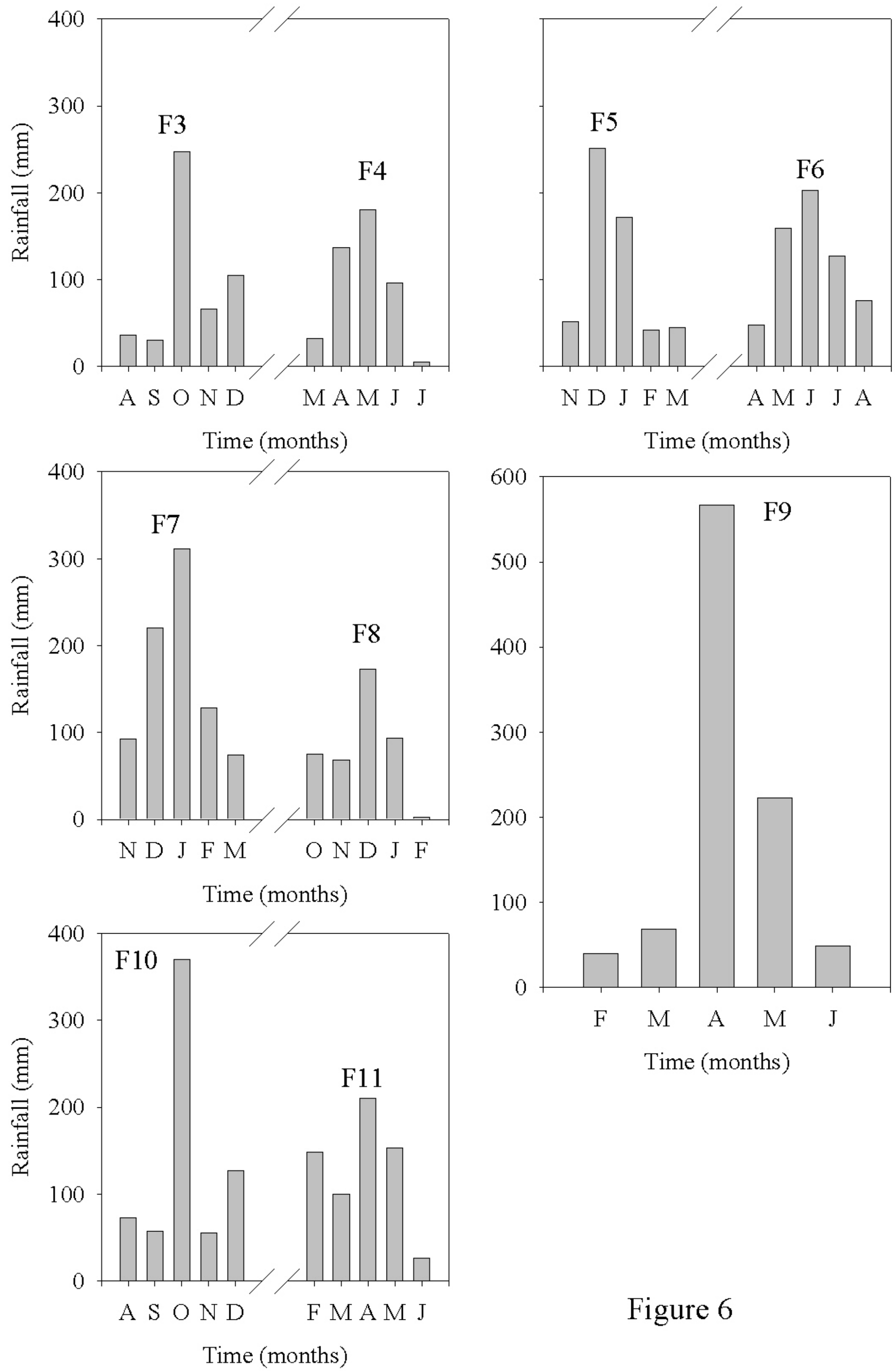

Rainfall (mm)
Time (months)
F3
F4
A S O N D
M A M J J
F5
F6
N D J F M
A M J J A
F7
F8
N D J F M
O N D J F
F9
F M A M J
F10
F11
A S O N D
F M A M J

Figure 6

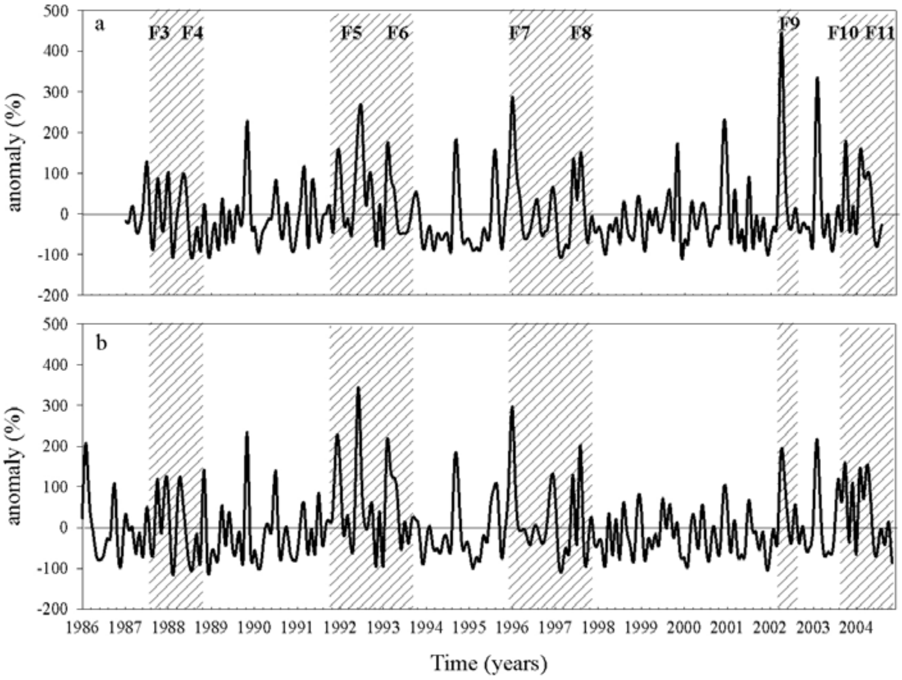

Figure 7

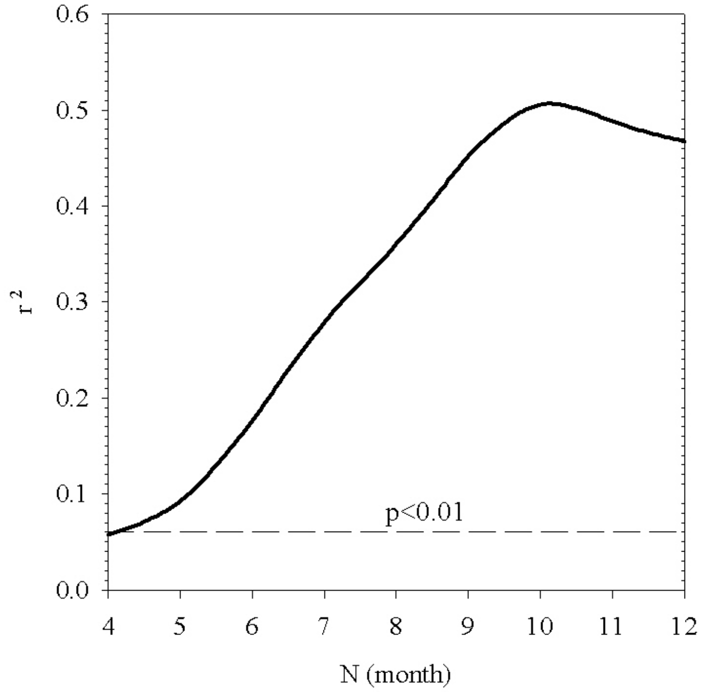

Figure 8

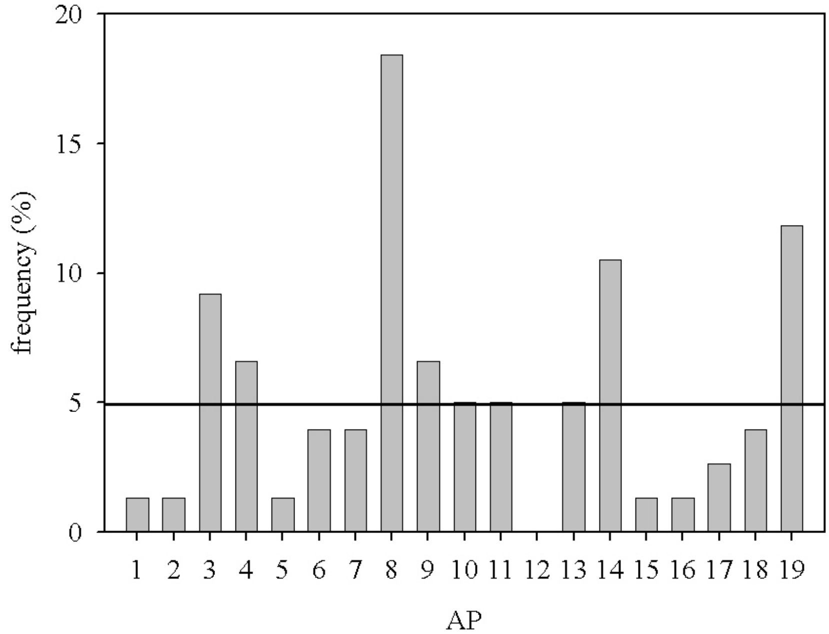

Figure 9

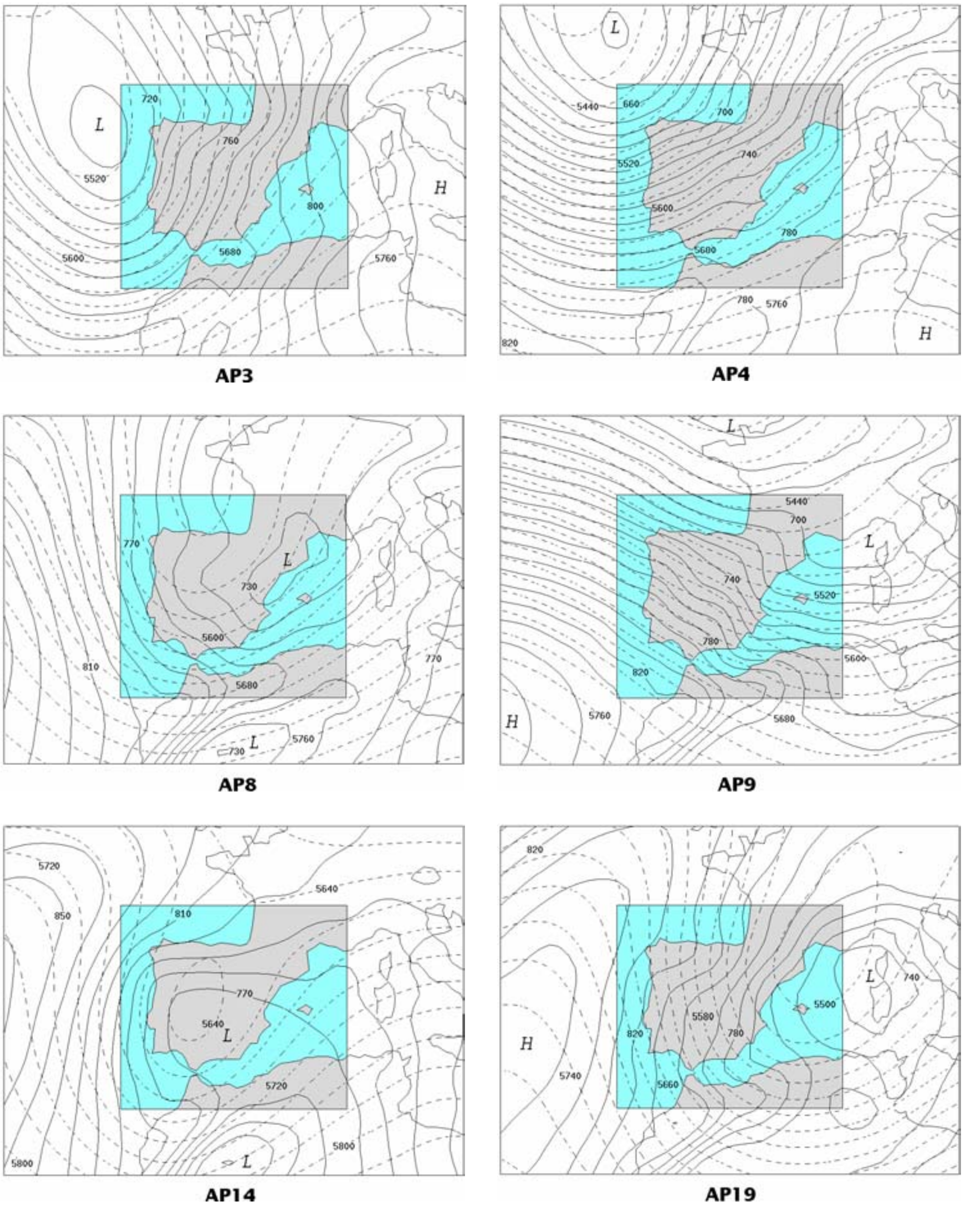

Figure 10

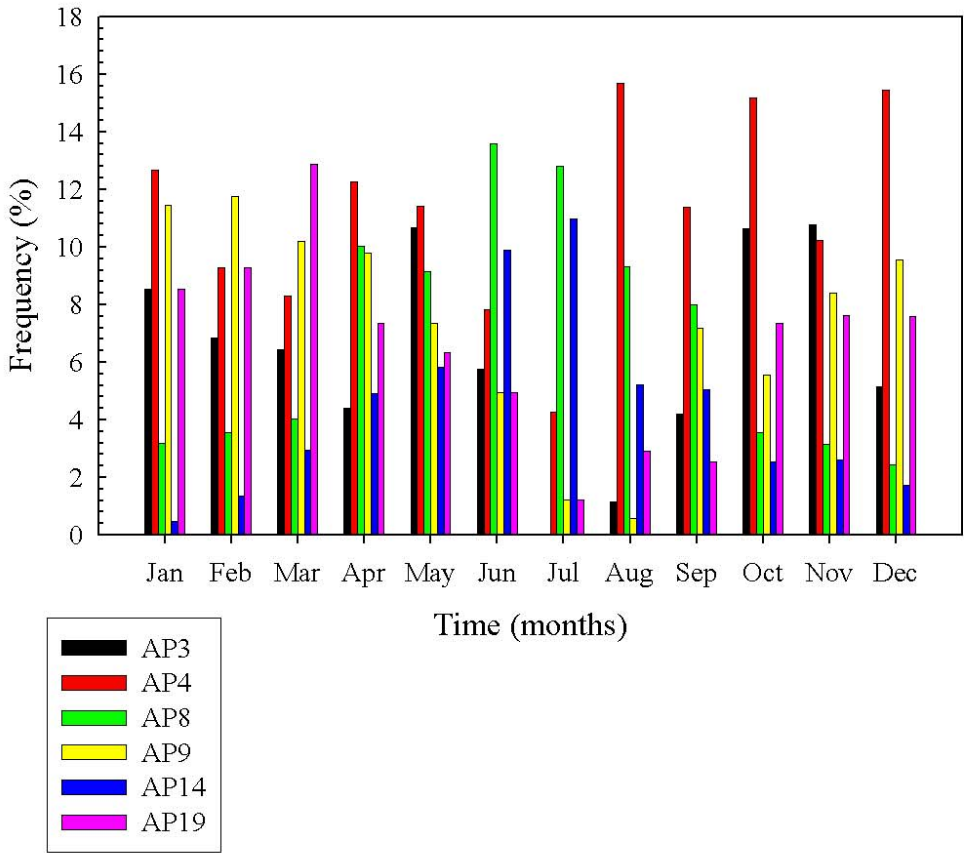
Frequency (%)
0
2
4
6
8
10
12
14
16
18
Jan
Feb
Mar
Apr
May
Jun
Jul
Aug
Sep
Oct
Nov
Dec
Time (months)
AP3
AP4
AP8
AP9
AP14
AP19

Figure 11

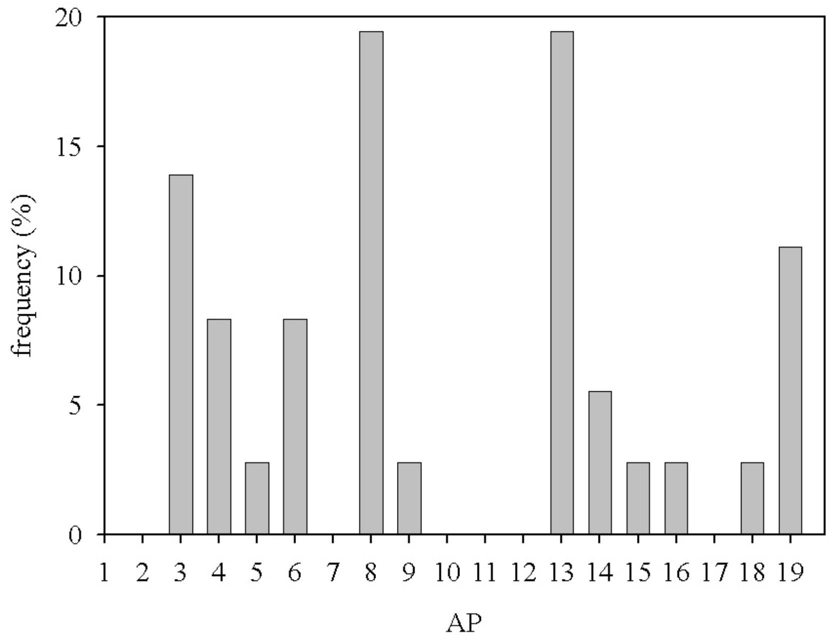

Figure 12